

# A Plasmonic DNAzyme Strategy for Point-of-Care Genetic Detection of Infectious Pathogens\*\*

Kyryl Zagorovsky and Warren C. W. Chan\*

The development of simple, cost-effective, sensitive, and specific point-of-care (POC) diagnostics represents a major challenge in the 21st century.<sup>[1]</sup> The spread of infectious diseases has caused significant losses in the global economy and in lives. One method to control the spread of diseases is to detect the pathogens early and to administer the proper treatment or quarantine.<sup>[2]</sup> Detection of DNA as biomarkers is currently a widely used technique for pathogen detection.<sup>[3]</sup> Quantitative PCR (qPCR) is the method of choice, because it includes an enzymatic signal amplification step to achieve highly sensitive and specific detection of genetic targets.<sup>[4]</sup> However, qPCR requires expensive equipment and highly trained personnel, limiting the use of this technique to medical laboratories. There is a strong need to develop cheaper and simpler DNA detection methods.<sup>[5]</sup> Herein, we combined colorimetric coupling of surface plasmons of gold nanoparticles with DNAzyme signal amplification technology to create a fast and simple detection method for genetic targets with a simple colorimetric readout. The novelty of this study is the integration of these two emerging technologies for point-of-care analysis of infectious disease targets.

A DNAzyme is a synthetic DNA enzyme that can catalyze the cleavage of another nucleic acid molecule.<sup>[6–8]</sup> Because the catalysis is carried out with multiple turnovers, the DNAzyme introduces an amplification step into the experimental setup.<sup>[9]</sup> This amplification is performed without the need for protein components, which are costly and have low thermal stability. Although they were initially designed to detect Pb<sup>2+</sup> and other divalent cations,<sup>[10–19]</sup> a number of modifications have been reported that allow DNAzymes to detect biomolecular targets.<sup>[9,20–27]</sup> Two main approaches were used to detect genetic targets: the first method uses competitive activation of a peroxidase-mimicking DNAzyme,

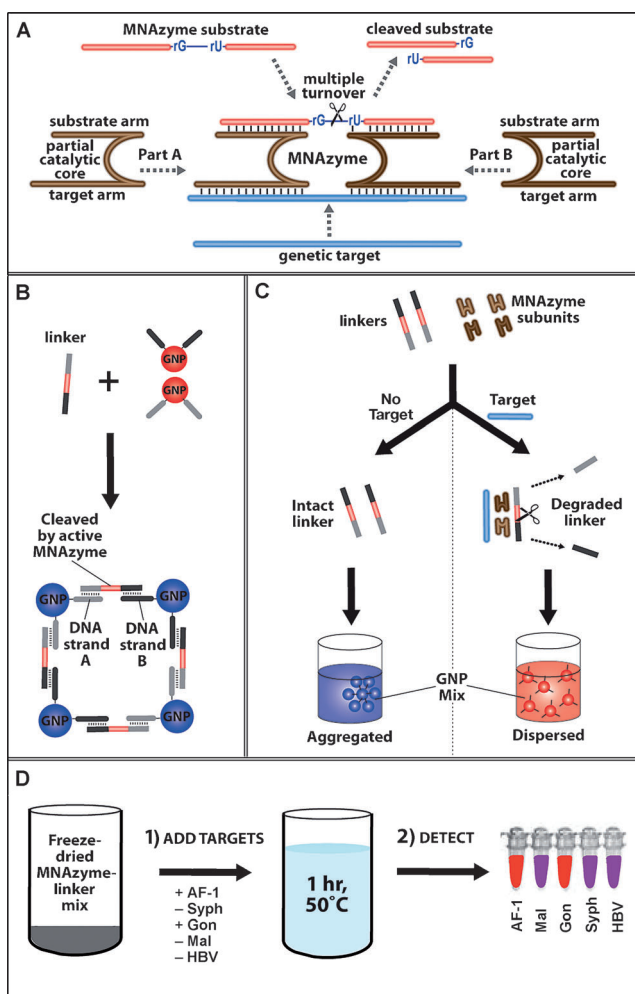
which can catalyze the production of a colorimetric or chemiluminescent product.<sup>[28]</sup> In the second, more sensitive approach, a similar strategy was used by a number of groups to detect genetic targets by splitting the DNAzyme into two inactive components, which could be reactivated by binding to a target.<sup>[9,23–25,29]</sup> However, these studies used fluorescence as the readout, which is not an optimal detection method for POC applications because it requires access to a fairly complex fluorometer. An alternative method using the colorimetric readout of gold nanoparticles (GNPs) has been reported for detection of metal ions, adenosine, and cocaine.<sup>[10–14,16–18,20,21]</sup> The wavelength at which GNPs absorb light is dependent on whether they are in a monodisperse or aggregated state.<sup>[30]</sup> Because it is easy to distinguish between the monodisperse or aggregated GNP solutions by their respective red or purple colors, this approach provides clear colorimetric results that can be seen by the naked eye.<sup>[31]</sup> In this study, we combined DNAzyme technology with GNPs to give a simple point-of-care diagnostic technique that can be used in remote settings.<sup>[32,33]</sup>

Figure 1 demonstrates the details of the experimental setup. Two sets of GNPs (13 nm), GNP-A and GNP-B, were functionalized with 5'-thiol-modified Agg/A (DNA aggregation (Agg) strand A) or 3'-thiol-modified Agg/B (DNA aggregation (Agg) strand B) DNA, respectively.<sup>[34]</sup> The linker strand was designed to have its 5'-end complementary to the 3'-end of Agg/A, and its 3'-end complementary to the 5'-end of Agg/B. The linker can cross-link GNP-A and GNP-B through hybridization, forming an aggregate network of GNPs (Figure 1B). The close proximity of the cross-linked GNPs causes coupling of their individual localized plasmon fields, leading to a shift in their absorbance to a longer wavelength, and the color of the solution changes from red to purple. In addition, the linker strand includes a substrate sequence that can be cleaved by a multicomponent nucleic acid enzyme (MNAzyme), which is one of the reported DNA-responsive DNAzymes. Initially in an inactive state, the binding of the target to the sensor bridges parts A and B of the MNAzyme, forming the active structure, which can then hybridize to the substrate sequence and catalyze its cleavage (Figure 1A).<sup>[9]</sup> The substrate sequence comprises DNA bases with two RNA nucleotides, which are required for cleavage, in the middle.<sup>[6]</sup> MNAzymes can be made responsive to any genetic target simply by changing the DNA bases of the sensor arms. The sequence of the substrate arms ensures the specificity of MNAzymes to a particular substrate, so that multiple MNAzyme–substrate pairs can be used in the same assay without cross-reactivity. MNAzymes use Mg<sup>2+</sup> as their divalent cation and have optimal activity at 50 °C. Among the three reported DNA-responsive bipartite DNAzymes, we

[\*] K. Zagorovsky, Dr. W. C. W. Chan  
Institute of Biomaterials and Biomedical Engineering,  
Terrence Donnelly Centre for Cellular and Biomolecular Research,  
Chemistry, Chemical Engineering, Materials Science and Engineering,  
University of Toronto  
160 College Street, Room 450, Toronto, ON, M5S3E1 (Canada)  
E-mail: warren.chan@utoronto.ca

[\*\*] The authors acknowledge the Canadian Institute of Health Research (MOP93532) and Natural Science and Engineering Research Council (CRDPCG411601) for funding through the CHRP program (CPG-112321), Canadian Foundation for Innovation, and Ministry of Research and Innovation. The authors thank Mr. Leo Chou for pertinent discussions, and Dr. Anu Rebbapragada and Mr. Stephen Perusini for designing the targets for *N. gonorrhoeae* detection.

Supporting information for this article (experimental details) is available on the WWW under <http://dx.doi.org/10.1002/anie.201208715>.



**Figure 1.** A) Mechanism of MNzyme catalysis. Adapted from Ref. [9] with permission. Copyright 2009, American Chemical Society. B) GNP aggregate formation. The linker hybridizes to DNA strands A and B, cross-linking the two sets of GNPs together and turning the solution purple. C) Outline of the MNzyme assay. Target-activated MNzymes degrade the linker DNA, preventing the formation of GNP aggregates. In the absence of the target, the linkers remain intact and cross-link the GNPs, as in (B); the solution turns purple. D) Scheme depicting how the assay can be conducted at the point-of-care to analyze multiple targets in parallel.

chase to work with the MNzyme, because it has the highest catalytic rate.<sup>[9,24,25,29]</sup>

This genetic sensing assay was implemented in a simple two-step system (Figure 1C). In the amplification step, a buffered mix of MNzymes and linkers is added to the sample solution and incubated at 50 °C for one hour. If target sequences are present, they bind and activate the MNzymes. Each active MNzyme in turn catalyzes cleavage of multiple linkers, which effectively translates into signal amplification. In the detection step, a mix of GNP-A and GNP-B is added to the sample solution. In the absence of the genetic target, intact linkers interact with the GNPs to form an aggregate network, turning the solution purple. In contrast, the presence of the genetic target results in linker degradation. GNP-A and GNP-B do not get cross-linked and the solution remains red.

For a readout, we used the change in solution color when 3  $\mu\text{L}$  of solution was spotted onto a thin-layer chromatography (TLC) plate.<sup>[31]</sup> TLC plates intensify the difference in color allowing for more sensitive visual detection and can be stored for later viewing. A measurement of the UV/Vis spectroscopic shift of absorbance was used to confirm these results.<sup>[35]</sup>

One critical parameter to optimize for the assay is the amount of linker strand used. For a given GNP concentration, there is a minimum linker concentration that is able to cross-link the GNPs sufficiently to cause visual aggregation. With such a linker/GNP ratio, even if a small proportion of the linker strands is cleaved by the MNzymes, this should have an effect on the GNP cross-linking and the color of the solution. Therefore, minimizing the linker concentration effectively maximizes the sensitivity of the assay. Optimization results are presented in Figure 2A. The assay setup

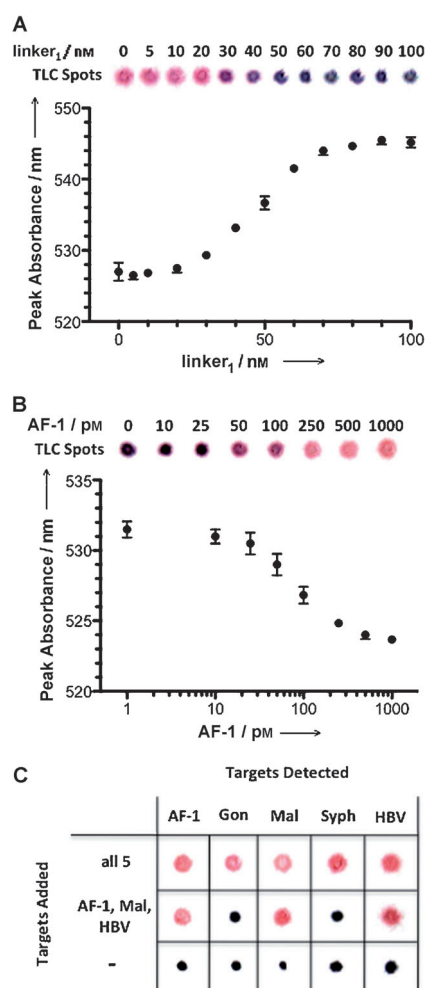


**Figure 2.** A) Optimization of linker<sub>1</sub> concentration. B) Sensitivity of detecting AF-1. A,B) Top: colorimetric readout on a TLC plate. Bottom: shift in the wavelength of the absorbance peak. Data are based on three replicates; Error bars = standard error. C) Parallel detection of five targets: AF-1 and genetic sequences from *N. gonorrhoeae* (Gon) and *T. pallidum* (Syph) bacteria, malarial parasite *P. falciparum* (Mal), and HBV virus. The color of the spot indicates presence (red) or absence (purple/black) of the target. Images were adjusted for contrast and brightness.

matched the experimental condition of the MNAzyme<sub>1</sub> assay, but lacked the genetic target to prevent linker<sub>1</sub> degradation. As the amount of linker<sub>1</sub> was increased from 0 to 100 nM, there was a sigmoidal shift in the absorption peak,  $\lambda_{\text{Peak}}$ , from 527 nm to 546 nm, indicating an increase in the size of the GNP aggregates. The color of the TLC spot followed a similar, but steeper, sigmoidal trend. The spots appear red up to 20 nM, then gradually shift to dark purple/black at 50 nM, and remain unchanged for higher concentrations. Based on both the color change and shift in the absorbance peak we chose 40 nM as the optimal linker<sub>1</sub> concentration.

Next, we carried out the MNAzyme assay outlined in Figure 1 to detect AF-1, which refers to the model genetic target designed to facilitate the assembly of a catalytically active MNAzyme complex. As determined previously, 40 nM linker was used, and we assayed AF-1 from 0  $\mu\text{M}$  to 1 nM (Figure 2B). Similar to Figure 2A, spectroscopic data showed a sigmoidal, but decreasing trend in  $\lambda_{\text{Peak}}$ . Absorbance peaks shifted from 533 nm for the sample without AF-1 to 523 nm for 1 nM of target. The color of the TLC spots followed a similar trend, remaining purple from 0  $\mu\text{M}$  to 25  $\mu\text{M}$  AF-1, then gradually shifting to red at 500  $\mu\text{M}$  and 1000  $\mu\text{M}$ . Both spectroscopic and spot color data established the limit of detection of this assay at 50  $\mu\text{M}$ . This sensitivity is slightly lower than the 5  $\mu\text{M}$  reported for the fluorescence readout assay.<sup>[9]</sup>

Interestingly, if the linker is chosen as the target instead of AF-1, the experiment from Figure 2A matches the original MNAzyme-free direct DNA-detection assay reported by Mirkin and co-workers (we confirmed that 50 °C and one hour incubation does not affect the assay results; Supporting Information, Figure S1).<sup>[31]</sup> Based on Figure 2A, our assay has a detection sensitivity of approximately 30 nM. Therefore, inclusion of the MNAzyme signal amplification increases detection sensitivity by a factor of 600.

We further investigated whether the colorimetric MNAzyme assay could detect multiple targets in parallel (Figure 1D). We chose four additional targets corresponding to genetic sequences for gonorrhea (Gon)<sup>[36]</sup> and syphilis (Syph)<sup>[37]</sup> bacteria, malaria parasite (Mal),<sup>[38]</sup> and hepatitis B virus (HBV).<sup>[39]</sup> These infectious diseases are prevalent in both the developed and developing world, and can cause severe health problems and death in patients that are not properly diagnosed and treated. To detect these targets, four new MNAzyme-linker-GNP sets were developed, each specific for one of the targets. For example, MNAzyme<sub>Mal</sub> had substrate arms specific for Linker<sub>Mal</sub>, and sensor arms complementary to Mal target, but not the other linker sequences or targets. Linker<sub>Mal</sub>, in turn, could aggregate GNP-A<sub>Mal</sub> and GNP-B<sub>Mal</sub>, but not other GNP pairs. Another modification introduced to the assay was lyophilization of the assay components. In this form, the reagents remain stable during storage and transport, making them well suited for POC testing.<sup>[40]</sup>

In the first step of the assay, a solution containing the genetic targets was added to a reaction tube containing a mixture of five sets of MNAzyme-Linker pairs, and incubated at 50 °C for one hour. When AF-1 and Gon targets were present, they activated MNAzyme<sub>AF-1</sub> and MNA-

zyme<sub>Gon</sub>, which in turn degraded linker<sub>AF-1</sub> and linker<sub>Gon</sub>. The other three linkers remained intact. In the second step, 10  $\mu\text{L}$  of the MNAzyme-linker-target solution was transferred to five detection tubes, each containing a target-specific GNP pair. Any linkers that remained uncleaved caused aggregation of the corresponding GNP pairs, turning solution purple. In contrast, linkers cleaved by target-activated MNAzymes were not able to cross-link the associated GNP pairs, and solution remained red. In the example described above, only the mixtures in AF-1- and Gon-specific detection tubes would remain red. Following this method we successfully detected all five targets simultaneously (Figure 2C). In addition, the assay with lyophilized components was used to correctly identify AF-1, Mal, and HBV sequences in a sample mixture that contained three out of the five targets.

In summary, the MNAzyme-GNP assay provides a simple and fast colorimetric method for detection of genetic targets of bacterial, viral, and parasitic origins with 50  $\mu\text{M}$  sensitivity without the need for purification and separation steps. The results can be archived when spotted on TLC plates. To our knowledge, this is the first report of combining a multi-component DNA-responsive DNAzyme with colorimetric detection of gold nanoparticles. This assay can detect multiple genetic sequences in parallel and could be easily applied to other nucleic acid targets. The color-based readout does not require any complex equipment and uses stable and cost-effective reagents, making this approach particularly suitable for POC testing. Furthermore, it is difficult to identify specific requirements for the analytical sensitivity of a pathogen because the sensitivity may vary based on the treatment strategy and whether there is a single or co-infection. Improved sensitivity could be achieved by modifying the size of the nanoparticles, modifying the chemistry used to attach the DNA to the GNPs, varying the length of MNAzyme/linker or target sequences,<sup>[41]</sup> or by combining the fast catalytic rate of MNAzymes and colorimetric plasmonic readout with the sensitive protein-free autocatalytic DNAzyme approach demonstrated by Willner and co-workers.<sup>[23,42]</sup> Furthermore, in a complete POC system, it is likely that extra components that can extract the genetic targets of interest would need to be included. Such methods have already been developed for isolating targets from blood and stool samples.<sup>[43–45]</sup> Finally, synthetic genetic targets are commonly used as the first step in the assessment of new POC devices. In the next step, further evaluation using clinical samples is required to assess clinical specificity and sensitivity prior to real-world use.

Received: October 30, 2012

Revised: December 24, 2012

Published online: February 10, 2013

**Keywords:** biosensors · DNAzymes · DNA recognition · nanoparticles · surface plasmon resonance

[1] S. Binder, A. M. Levitt, J. J. Sacks, J. M. Hughes, *Science* **1999**, 284, 1311–1313.

[2] T. S. Hauck, S. Giri, Y. Gao, W. C. W. Chan, *Adv. Drug Delivery Rev.* **2010**, 62, 438–448.

- [3] J. Weile, C. Knabbe, *Anal. Bioanal. Chem.* **2009**, *394*, 731–742.
- [4] M. J. Espy, J. R. Uhl, L. M. Sloan, S. P. Buckwalter, M. F. Jones, E. A. Vetter, J. D. C. Yao, N. L. Wengenack, J. E. Rosenblatt, F. R. Cockerill III, T. F. Smith, *Clin. Microbiol. Rev.* **2006**, *19*, 165–256.
- [5] S. Giri, E. A. Sykes, T. L. Jennings, W. C. W. Chan, *ACS Nano* **2011**, *5*, 1580–1587.
- [6] K. Schlosser, Y. Li, *ChemBioChem* **2010**, *11*, 866–879.
- [7] S. W. Santoro, G. F. Joyce, *Proc. Natl. Acad. Sci. USA* **1997**, *94*, 4262–4266.
- [8] R. R. Breaker, G. F. Joyce, *Chem. Biol.* **1994**, *1*, 223–229.
- [9] E. Mokany, S. M. Bone, P. E. Young, T. B. Doan, A. V. Todd, *J. Am. Chem. Soc.* **2010**, *132*, 1051–1059.
- [10] W. Zhao, J. C. F. Lam, W. Chiuman, M. A. Brook, Y. Li, *Small* **2008**, *4*, 810–816.
- [11] J. Liu, Y. Lu, *J. Am. Chem. Soc.* **2004**, *126*, 12298–12305.
- [12] J. Liu, Y. Lu, *J. Am. Chem. Soc.* **2003**, *125*, 6642–6643.
- [13] J. Liu, Y. Lu, *Org. Biomol. Chem.* **2006**, *4*, 3435–3441.
- [14] D. Mazumdar, J. Liu, G. Lu, J. Zhou, Y. Lu, *Chem. Commun.* **2010**, *46*, 1416–1418.
- [15] X. Miao, L. Ling, X. Shuai, *Chem. Commun.* **2011**, *47*, 4192–4194.
- [16] H. Wei, B. Li, J. Li, S. Dong, E. Wang, *Nanotechnology* **2008**, *19*, 095501.
- [17] J. H. Lee, Z. Wang, J. Liu, Y. Lu, *J. Am. Chem. Soc.* **2008**, *130*, 14217–14226.
- [18] Z. Wang, J. H. Lee, Y. Lu, *Adv. Mater.* **2008**, *20*, 3263–3267.
- [19] J. Li, Y. Lu, *J. Am. Chem. Soc.* **2000**, *122*, 10466–10467.
- [20] J. Liu, Y. Lu, *Anal. Chem.* **2004**, *76*, 1627–1632.
- [21] J. Liu, Y. Lu, *J. Fluoresc.* **2004**, *14*, 343–354.
- [22] D. Wang, B. Lai, D. Sen, *J. Mol. Biol.* **2002**, *318*, 33–43.
- [23] F. Wang, J. Elbaz, R. Orbach, N. Magen, I. Willner, *J. Am. Chem. Soc.* **2011**, *133*, 17149–17151.
- [24] F. Wang, J. Elbaz, C. Teller, I. Willner, *Angew. Chem.* **2011**, *123*, 309–313; *Angew. Chem. Int. Ed.* **2011**, *50*, 295–299.
- [25] Y. V. Gerasimova, E. Cornett, D. M. Kolpashchikov, *ChemBioChem* **2010**, *11*, 811–817.
- [26] S. Sando, A. Narita, T. Sasaki, Y. Aoyama, *Org. Biomol. Chem.* **2005**, *3*, 1002–1007.
- [27] S. Sando, T. Sasaki, K. Kanatani, Y. Aoyama, *J. Am. Chem. Soc.* **2003**, *125*, 15720–15721.
- [28] J. Kosman, B. Juskowiak, *Anal. Chim. Acta* **2011**, *707*, 7–17.
- [29] D. M. Kolpashchikov, *ChemBioChem* **2007**, *8*, 2039–2042.
- [30] M. Quinten, U. Kreibitz, D. Schönauer, L. Genzel, *Surf. Sci.* **1985**, *156*, 741–750.
- [31] R. Elghanian, J. J. Storhoff, R. C. Mucic, R. L. Letsinger, C. A. Mirkin, *Science* **1997**, *277*, 1078–1081.
- [32] C. D. Medley, J. E. Smith, Z. Tang, Y. Wu, S. Bamrungsap, W. Tan, *Anal. Chem.* **2008**, *80*, 1067–1072.
- [33] K. Sato, K. Hosokawa, M. Maeda, *Nucleic Acids Res.* **2005**, *33*, e4.
- [34] S. J. Hurst, A. K. R. Lytton-Jean, C. A. Mirkin, *Anal. Chem.* **2006**, *78*, 8313–8318.
- [35] J. J. Storhoff, R. Elghanian, R. C. Mucic, C. A. Mirkin, R. L. Letsinger, *J. Am. Chem. Soc.* **1998**, *120*, 1959–1964.
- [36] R. Rossau, L. Heyndrickx, H. Van Heuverswyn, *Nucleic Acids Res.* **1988**, *16*, 6227.
- [37] J. Burstain, E. Grimprel, S. Lukehart, M. Norgard, J. Radolf, *J. Clin. Microbiol.* **1991**, *29*, 62–69.
- [38] A. R. Bharti, K. P. Patra, R. Chuquiyaui, M. Kosek, R. H. Gilman, A. Llanos-Cuentas, J. M. Vinetz, *Am. J. Trop. Med. Hyg.* **2007**, *77*, 444–446.
- [39] D. Paraskevis, A. Beloukas, C. Haida, A. Katsoulidou, Z. Moschidis, H. Hatzitheodorou, A. Varaklioti, V. Sypsa, A. Hatzakis, *Viol. J.* **2010**, *7*, 57.
- [40] W. Abdelwahed, G. Degobert, S. Stainmesse, H. Fessi, *Adv. Drug Delivery Rev.* **2006**, *58*, 1688–1713.
- [41] Y. Gao, W. L. Stanford, W. C. W. Chan, *Small* **2011**, *7*, 137–146.
- [42] S. Shimron, F. Wang, R. Orbach, I. Willner, *Anal. Chem.* **2012**, *84*, 1042–1048.
- [43] S. R. Jangam, D. H. Yamada, S. M. McFall, D. M. Kelso, *J. Clin. Microbiol.* **2009**, *47*, 2363–2368.
- [44] A. V. Govindarajan, S. Ramachandran, G. D. Vigil, P. Yager, K. F. Boehringer, *Lab Chip* **2012**, *12*, 174–181.
- [45] A. G. Freifeld, K. A. Simonsen, C. S. Booth, X. Zhao, S. E. Whitney, T. Karre, P. C. Iwen, H. J. Viljoen, *J. Mol. Diagn.* **2012**, *14*, 274–279.